Utrecht University

Chaotic Behavior in Continuous Economic Models

BACHELOR THESIS

Author:
Eppo van der Heijden
3882632
Utrecht University

Supervised by:
Prof. dr. ir. Jason Frank
Utrecht University

June 9, 2017

Abstract

In economic chaos theory, results often follow from the analysis of discrete dynamical systems. In this thesis, we review three methods for identifying chaos in continuous dynamical systems: the analysis of Lyapunov exponents, methods for computing unstable periodic orbits and the 0-1 test for chaos. The results for three economic models do not seem to be in agreement for the different methods.

Contents

1 Introduction

1.1 Chaos in economics

In today's economy, many complex phenomena such as irregular fluctuations and unpredictable market transitions may arise. The financial-economic crisis that started in 2007 is an example of the devastating effects these events can have on the worldwide market. Policymakers are faced with the question to respond to these fluctuations. In order to do so, it is important to understand the underlying dynamics and phenomena that may appear with such dynamics.

We can distinguish between exogenous and endogenous "shocks" that may have influence on an economic system. In the early days of the study of economic dynamical systems, which we can roughly date back to the 1930s, the exogenous effects on an inherently stable economic system were often investigated. In the 1940s and 1950s, this linear stability was criticized because it did not give an economic explanation of observations. They were countered by the nonlinear business cycle models, but because these models also did not suffice, a new theory of rational expectations was set up in the 1960s. In mathematics and physics, deterministic chaos was discovered in the 1960s. The application of this new chaos theory would lead to a definite choice for the endogenous effects as the focus of research in economic systems. Hommes explains this internal variability with the idea of a behavioral theory of heterogeneous expectations [7].

However, the models that he uses are low-dimensional dynamical systems with discrete time steps. This makes the models easy to understand and reproduce, but the viability of discrete-time economics can be questioned. It is also known that chaos can occur in discrete dynamical systems of all dimensions, whereas chaos in continuous-time dynamical systems can only occur for dimension at least three. Hence, chaos should not be endogenous to continuous economic models with one or two dimensions, unless discrete forcing plays a role.

1.2 Discrete versus continuous dynamical systems

The models Hommes uses are dynamical systems with discrete time step. They assume a feedback system with a fixed time step. Even though economic transactions do not take place continuously, in general they will not take place with a fixed time step. These transactions will overlap in a random way, and only in rare circumstances one can define a 'natural period' [12]. Furthermore, because trades on the financial market can be made everywhere and always, the continuity assumption of the economy has become an even stronger 'approximation' of the reality.

As we mentioned before, chaotic behavior can occur in one-dimensional discrete systems, whereas it can only occur in continuous systems with at least three dimensions. The assumption of chaotic behavior in complex economic systems is therefore more satisfied by showing chaos in continuous models.

To study the chaotic behavior of continuous dynamical systems, we will focus

on the dynamics upon the strange attractor of the system. This attractor can be informally defined as the invariant set to which most orbits of the systems tend.

1.3 Deterministic chaos

We will restrict ourselves to the study of deterministic chaos described by ordinary differential equations. Deterministic chaos can be characterized informally by the following three properties [2]:

1. sensitive dependence on initial conditions
2. dense unstable periodic orbits
3. topological mixing on an attractor

In this thesis, we review three methods for identifying chaos in continuous dynamical systems: analysis of Lyapunov exponents (2.1), methods for computing unstable periodic orbits (2.2) and the so-called 0-1 test for chaos (2.3). The first two of these can be used to identify sensitive dependence on initial conditions, the second to find unstable periodic orbits and the third of these seeks to identify non(quasi-)periodic behavior.

2 Methods

2.1 Lyapunov exponents

2.1.1 Interpretation

Lyapunov exponents are concerned with the asymptotic growth speed of solutions of linearized dynamical systems. They can be considered informally as the time-averaged eigenvalues of a non-autonomous systems of differential equations. Let

$$y'(t) = f(t, y(t)), y(t) \in \mathbb{R}^d, f : \mathbb{R} \times \mathbb{R}^d \to \mathbb{R}^d, \tag{1}$$

be a system of d differential equations. Define the Jacobian matrix of f by

$$A(t) = \big(A_{ij}(t)\big) := \Big(\frac{\partial f_i(t,y)}{\partial y_j}\Big), \quad i,j = 1,\dots,d. \tag{2}$$

Let $Y(t) \in \mathbb{R}^{d\times d}$ satisfy the matrix differential equation

$$Y'(t) = A(t)Y(t), \;\; Y(0) = Y_0 \;\; \text{invertible}, \tag{3}$$

then $Y(t)$ is called a fundamental matrix solution. Now let

$$\lambda_i := \limsup_{t\to\infty} \frac{1}{t} ||Y(t)e_i||, \tag{4}$$

where e_i are the canonical coordinate vectors, be such that $\sum_i \lambda_i$ is minimal over all Y_0. We shall call these d quantities the Lyapunov exponents of (1).
In particular, for a system

$$y'(t) = B(t)y(t), y(t) \in \mathbb{R}^d, f : \mathbb{R} \times \mathbb{R}^d \to \mathbb{R}^d, \tag{5}$$

such that $B(t)$ is upper triangular for all t, i.e., all entries below the main diagonal are zero, we can define the Lyapunov exponents as

$$\lambda_i = \lim_{t\to\infty} \frac{1}{t} \int_0^t B_{ii}(s)ds, \tag{6}$$

assuming that $B(t)$ is bounded, continuous and regular. For computational reasons, this definition is preferred over (4). For a general system, we should therefore find a continuous change of variables such that it can be written as (5).
The most common means of identifying chaos is to establish that at least one Lyapunov exponent is positive on the strange attractor.

2.1.2 QR factorization

The QR factorization of a real matrix Y is a decomposition

$$Y = QR, \tag{7}$$

where Q satisfies $Q^TQ = I$, i.e., Q is orthonormal, and R is upper triangular with positive diagonal. If Y is non-singular, this decomposition is unique. There are several methods for explicitly computing the decomposition, but we shall use the *modified Gram-Schimdt algorithm* in this thesis. For more details, see, for instance, [4].

2.1.3 Practical computation

Let Y be a fundamental matrix solution of (1). We then factorize this solution by the Gram-Schmidt procedure: $Y(t) = Q(t)R(t)$, where $Q \in \mathbb{R}^{d\times d}$ is orthonormal and R is upper triangular. Define the matrix $S(t) = Q(t)^T\dot{Q}(t)$. Then by differentiating both sides of the orthonormality relation $Q(t)^TQ(t) = I$,

$$\frac{d}{dt}(Q(t)^TQ(t)) = \dot{Q}(t)^TQ(t) + Q(t)^T\dot{Q}(t) = \frac{d}{dt}I = 0,$$

we see that S is skew-symmetric. Substituting the QR factorization is (3) gives

$$\dot{Q}R + Q\dot{R} = AQR. \tag{8}$$

We can split this equation into separate differential equations for R and Q. At first, we multiply by Q^T from the left. This yields the equation

$$\dot{R} = BR, \tag{9}$$

with

$$B(t) = Q(t)^TA(t)Q(t) - S(t). \tag{10}$$

Now because R and $\dot{R}$ are upper triangular, it follows that $B = \dot{R}R^{-1}$ is also upper triangular. By construction, one sees that the lower triangular part of S will cancel out the lower triangular part of Q^TAQ. So because S is skew-symmetric, we can fully specify its components:

$$S_{ij} = \begin{cases} (Q^T AQ)_{ij}, & i > j, \\ 0, & i = j, \\ -S_{ji}, & i < j, \end{cases} \tag{11}$$

We now multiply (8) by R^{-1} from the right, which gives the differential equation for Q:

$$\dot{Q} = AQ - Q\dot{R}R^{-1} = AQ - QB$$

$$\dot{Q} = AQ - Q\big(Q^T AQ - S\big)$$

$$\dot{Q} = \big(I - QQ^T\big)AQ + QS \tag{12}$$

We now see that by simultaneously solving the system of differential equations formed by (1), (9) and (12), we can use the definition of B as in (10) to compute the Lyapunov exponents in definition (6). This computation is implemented simultaneously with solving the system of differential equations to see the convergence of the Lyapunov exponents in time. All these computations are done with a fourth order Runga-Kutta method unless mentioned otherwise.

2.1.4 Attractor dimension

The Lyapunov exponents can be scaled by rescaling time. It is therefore useful to consider a quantitative characterization that accounts for the relative strength of the positive Lyapunov exponent(s). Let the Lyapunov exponents be labeled such that $\lambda_1 \geq \lambda_2 \geq \cdots \geq \lambda_d$ and let k be the index for which

$$\lambda_1 + \cdots + \lambda_k > 0 \quad \text{and} \quad \lambda_1 + \cdots + \lambda_{k+1} < 0.$$

We will calculate the Lyapunov dimension D_L as defined by Kaplan and Yorke [8]:

$$D_L = k + \frac{\lambda_1 + \cdots + \lambda_k}{|\lambda_{k+1}|}. \tag{13}$$

2.2 Unstable periodic orbits

Here we explain in more detail the Lindstedt-Poincaré technique to compute unstable periodic orbits as described by Viswanath in [13].
We want to numerically compute periodic solution of the (multidimensional) differential equation

$$\dot{x}(t) = f(x(t)). \tag{14}$$

If the period T is unknown, we can perform the time scaling $t \mapsto t/\omega$, where $\omega = 2\pi/T$. This leads to the differential equation

$$\omega\dot{x}(t) = f(x(t)), \tag{15}$$

where the corresponding periodic solution now has period 2π.

2.2.1 Fourier representation

We would now like to represent our periodic solution as a Fourier series:

$$x(t) = \sum_{k=-\infty}^{\infty} \hat{x}_k e^{ikt}. \tag{16}$$

As the solution now has period 2π, the Fourier coefficients $\hat{x}_k \in \mathbb{C}, k \in \mathbb{Z}$ are given by

$$\hat{x}_k = \int_{-\pi}^{\pi} x(t) e^{-ikt} dt.$$

To perform the numerical computation, we have to truncate the Fourier series to a finite number N. Assuming that our periodic solution is analytic, we can get an exponentially converging approximation as $N \to \infty$ by sampling the solution on a uniform grid with N grid points $x_j = x(j\Delta t), j = 0, 1, \ldots, N-1, \Delta t = 2\pi/N$. We can now apply discrete Fourier transformation to the grid function and its Fourier representation:

$$x_j = \frac{1}{N} \sum_{k=-N/2}^{N/2} \hat{x}_k e^{ijk\Delta t}, \quad \hat{x}_k = \sum_{j=0}^{N-1} x_j e^{-ijk\Delta t}. \tag{17}$$

The discrete Fourier transformation and its inverse can be effectively computed. The Fast Fourier Transformation (FFT) and the Inverse Fast Fourier Transformation (IFFT) are stable algorithms implemented in `MATLAB`, which allow computation of (17) in $\mathcal{O}(N \log N)$ operations.

Another advantage of this representation is that it allows us to compute the derivate of the function in an easy way:

$$x'(t) = \sum_{k=-\infty}^{\infty} ik\hat{x}_k e^{ikt}. \tag{18}$$

2.2.2 Newton's method

We now apply Newton's method to find a zero of the residual function

$$r(x(t), \omega) = f(x(t)) - \omega \dot{x}(t). \tag{19}$$

We now calculate $x(j\Delta t), j = 0, \ldots, N-1$ on a uniform grid, fill in these values in f_j and compute the FFT of f_j, $\hat{f}_k$, $k = -\frac{(N-1)}{2}, \ldots, \frac{(N-1)}{2}$, to find the Fourier representation of the residual:

$$\hat{r}_k = \hat{f}_k - ik\hat{x}_k.$$

Now assume we have a first guess $(x_0(t), \omega_0)$, then we can express the actual solution $(x(t), \omega)$ of a zero residual as a perturbation: $x(t) = x_0(t) + y(t)$ and $\omega = \omega_0 + d\omega$, where we dictate that $y(t)$ is periodic with period 2π. We can now linearize the residual around this guess to find an approximation:

$$r(x_0(t)+y(t),\omega_0+d\omega) \approx r(x_0(t),\omega_0) + A(t)y(t) - \omega_0\dot{y}(t) - d\omega\dot{x}_0(t), \quad (20)$$

where $A(t)$ is the Jacobian matrix of f, evaluated at the guess solution $x_0(t)$. With Newton's method, we now get a new guess $x_1(t) = x_0(t) + y(t)$ and $\omega_1 = \omega_0 + d\omega$, for which we repeat the procedure. The Lindstedt-Poincaré method is concerned with approximately finding a zero of (20).

2.2.3 Lindstedt-Poincaré method

For the l-th iteration of Newton's method, we have to solve the correction equation

$$\omega_l\dot{y}(t) = A(t)y(t) + r_l(t) - d\omega\dot{x}_l(t), \quad (21)$$

where $(x_l(t),\omega_l)$ is the starting guess and $r_l(t) := r(x_l(t),\omega_l)$, to find an approximate zero of the linearized residual. For notational reasons, we will now drop the subscript indicating the iteration. First, we consider the homogeneous part:

$$\omega\dot{y}(t) = A(t)y(t) \quad (22)$$

We can find a solution for every initial value $y(0) = y_0$ by solving the fundamental matrix equation

$$\omega\dot{Y}(t) = A(t)Y(t), \quad Y(0) = I, \quad (23)$$

for $Y \in \mathbb{R}^{d\times d}$. Then the solution of (22) is given by

$$y(t) = Y(t)y_0. \quad (24)$$

Now, we try a general solution of (21) in the form

$$y(t) = Y(t)y_0 + d\omega f_1(t) - f_2(t). \quad (25)$$

Filling in this solution in (21) and after collection terms, we see that $f_1(t)$ and $f_2(t)$ must satisfy

$$\omega\dot{f}_1(t) = A(t)f_1(t) + r(t), \quad (26)$$

$$\omega\dot{f}_2(t) = A(t)f_2(t) + \dot{x}(t). \quad (27)$$

We can let the initial conditions be given by $f_1(0) = f_2(0) = 0$. Now by solving (23), (26) and (27), we find the solution of (21) up to y_0 and $d\omega$. By demanding that $y(2\pi) = y_0$ and $f(x(0))^T y_0 = 0$, we ensure the solution is periodic and $d\omega$ is uniquely determined. Now we can again update the guess in (21) and repeat the algorithm.

2.3 The 0-1 test for chaos

The 0-1 test for chaos was developed in a series of papers by Gottwald and Melbourne to distinguish between regular and chaotic behavior in dynamical systems [5]. In contrast to the method of calculating Lyapunov exponents, the

0-1 test does not involve any preprocessing of the (discretized) data, use of Jacobian matrices or other processes that may influence the practical computation.

Given a time series $\phi(n)$, for $n = 1, \ldots, N$, of one of the variables of the system, let

$$p_c(n) = \sum_{j=1}^{n} \phi(j) \cos(jc), \quad q_c(n) = \sum_{j=1}^{n} \phi(j) \sin(jc) \tag{28}$$

for a random $c \in (\pi/5, 4\pi/5)$. From this, we calculate the time-averaged mean square displacement

$$M_c(n) = \frac{1}{N} \sum_{j=1}^{N} ([p_c(j+n) - p_c(j)]^2) + ([q_c(j+n) - q_c(j)]^2), \tag{29}$$

for $n \leq N/10$. The asymptotic growth rate K_c is given by

$$K_c = \lim_{n \to \infty} \frac{\log M_c(n)}{\log n}. \tag{30}$$

A significantly chaotic driving signal $\phi(n)$ is expected to behave approximately like a two-dimensional Brownian motion, causing (p, q) to undergo a random walk. In the (quasi)-periodic case, the behavior of (p, q) is expected to be bounded and to show symmetry.

We now repeat this procedure for 100 random values of $c \in (\pi/5, 4\pi/5)$, and we then plot $K = \text{median}(K_c)$ versus the number of iterations n to study the asymptotic behavior of K. For non-chaotic behavior, K will converge to 0 and for chaotic behavior, K will converge to 1.

Because we study continuous-time dynamical systems, we have to discretize the data to use this test. For all models, we take the last 10,000 points that are calculated in the Runga-Kutta method.

3 Application to test problems

In this section, we shall apply the described methods to identify chaos to the following models:

1. Lorenz-63 model
2. Medio model
3. Asada et al. model
4. H.-W. Lorenz model

The Lorenz-63 is not an economic model, but it is used to illustrate the methods and the familiar results. The non-chaotic Duffing oscillator model is used only to illustrate the Lindstedt-Poincaré method. We will introduce each model and explain its origin. The (projected) attractor of the model is also shown.

Duffing oscillator model
The Duffing oscillator, given by

$$\ddot{q} = -q - \epsilon q^3, \tag{31}$$

is a small perturbation of the linear oscillator. If we let $p = \dot{q}$, the system is transformed into a two-dimensional Hamiltonian system with $H(p,q) = \frac{p^2}{2} + \frac{q^2}{2} + \frac{\epsilon q^4}{4}$. We therefore know that every trajectory of this system of equations is a periodic orbit. We shall choose $\epsilon = 0.1$.

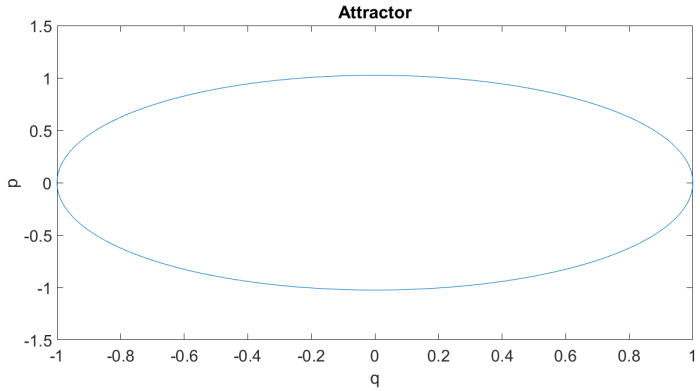

Figure 1: A trajectory of the Duffing oscillator in the (q,p)-plane for $\epsilon = 0.1$. It is calculated with $N = 20,000$ time steps of size $\Delta t = 0.01$ using a fourth order Runga-Kutta method. We see that it is a periodic orbit.

Lorenz-63 model
The differential equations

$$\dot{x} = \sigma(-x + y), \tag{32}$$

$$\dot{y} = -xz + rx - y, \tag{33}$$

$$\dot{z} = xy - bz, \tag{34}$$

with $\sigma = 10$, $r = 28$ and $b = \frac{8}{3}$, where studied by Edward Lorenz to illustrate irregular behavior in deterministic flow for relatively simple systems. It is one of the most studied systems, exhibiting chaotic behavior with a butterfly-like strange attractor.

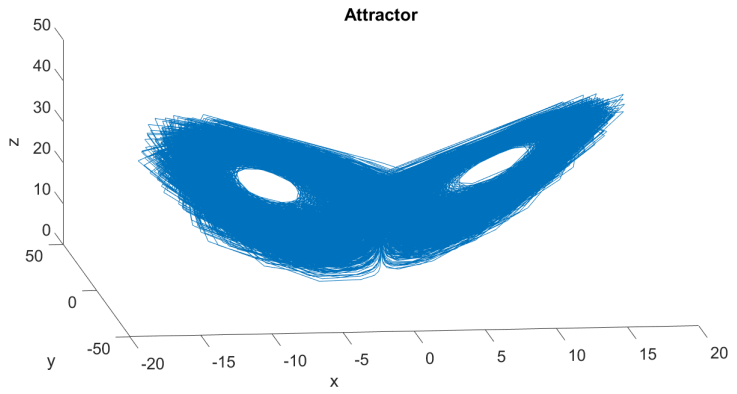

Figure 2: The Lorenz-63 attractor in the (x, y, z)-plane. It is calculated with $N = 20,000$ time steps with size $\Delta t = 0.1$ using a fourth order Runga-Kutta method. We see a butterfly-like attractor.

Medio model
The differential equations

$$\dot{x}_1 = 10rx_{10}(1 - x_{10}) - 10x_1, \tag{35}$$

$$\dot{x}_j = 10x_{j-1} - 10x_j, \quad j = 2, \ldots, 10, \tag{36}$$

for $r = 5$, form a ten-dimensional system that is equivalent to the model studied by Medio in [12,106]. It is seen as the continuous-time-equivalent of a discrete 'one-hump' function, in this case particularly the logistic map $x_{n+1} = rx_n(1 - x_n)$. The economic relevance of this system is not discussed in the paper by Medio: he uses the results of his computations to show the applicability of continuous-time system in the analysis of economic models, just as we do.

Asada et al. model
The system of differential equations governed by

$$\dot{u} = u\Big(\alpha_{uu}(u - \bar{u}) - \alpha_{ui}(i - \hat{p} - (\bar{i} - \bar{\pi})) + \alpha_{u\omega}\hat{\Omega}\Big), \tag{37}$$

$$\dot{\omega} = \kappa\omega\Big(\lambda_p(\beta_{we}(u - \hat{u}) - \beta_{w\omega}\hat{\Omega}) - \lambda_w(\beta_{pu}(u - \hat{u}) + \beta_{p\omega}\hat{\Omega})\Big), \tag{38}$$

$$\dot{\pi} = \beta_\pi(\hat{p} - \pi), \tag{39}$$

$$i = -\gamma_{ii}(i - \bar{i}) + \gamma_{ip}(\hat{p} - \bar{\pi}) + \gamma_{iu}(u - \bar{u}), \tag{40}$$

$$\hat{p} = \kappa\Big(\beta_{pu}(u - \bar{u}) + \beta_{p\omega}\hat{\Omega} + \kappa_p(\beta_{we}(u - \bar{u}) - \beta_{w\omega}\hat{\Omega})\Big) + \pi, \tag{41}$$

$$\hat{\Omega} = \log(\omega) - \log(\bar{\omega}), \tag{42}$$

is studied by Asada et al. as a model of a Keynesian macroeconomy, exhibiting complex dynamics [1]. If the $\hat{p}$- and $\hat{\Omega}$-equation are inserted in the four other equations, we find a four-dimensional autonomous system of differential equations in the four state variables u, the rate of capacity utilization of firms, ω,

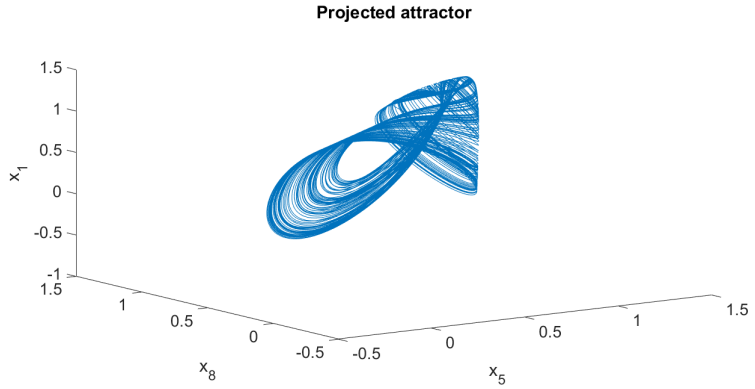

Figure 3: A projection of the Medio attractor onto the (x_5, x_8, x_1)-plane. It is calculated with $N = 20,000$ time steps with size $\Delta t = 0.01$ using a fourth order Runga-Kutta method. We see that the orbit follows an ring-like structure that is folded into itself.

the real wage, π, the inflationary climate and i the nominal rate of interest. Although the given set of parameters in the paper of Asada et al. is incomplete, we were able to find the missing values such that chaotic behavior seems to occur. The values of the chosen parameters are:

$$\beta_{pu} = 1, \beta_{p\omega} = 0.4, \lambda_p = 0.7, \beta_{we} = 0.8, \beta_{w\omega} = 0.4, \lambda_w = 0.3, \beta_\pi = 0.5,$$

$$\alpha_{uu} = 0.22, \alpha_{u\omega} = 0.1, \alpha_{ui} = 0.25, \gamma_{ii} = 0.1, \gamma_{ip} = 0.5, \gamma_{iu} = 1,$$

$$\kappa = 0.91, \bar{u} = 1.1, \bar{\omega} = 0.2, \bar{\pi} = 0.5 \text{ and } \bar{i} = 0.5,$$

with initial conditions $u_0 = 0.97$, $\omega_0 = 0.95$, $\pi_0 = 0.5$ and $\imath_0 = 0.5$. This model turned out to be mildly 'stiff': the fourth order explicit Runga-Kutta method did not give the desired results. We therefore integrate this model with a built-in `MATLAB`-function.

H.-W. Lorenz model

The six-dimensional system given by the equations

$$\dot{K}_i = I_i - \delta_i K_i, \tag{43}$$

$$\dot{Y}_i = \alpha(I_i - sY_i + \sum_{j>i} b_{ij} Y_i), \tag{44}$$

for $i, j = 1, 2, 3$, with

$$I_i = C 2^{\frac{-1}{(DY_i+\epsilon)^2}} + EY_i + A\Big(\frac{G}{K_i}\Big)^H, \tag{45}$$

is an adaptation of the macroeconomic business cycle model studied by Kaldor [9]. It models an economy with three sector i, where Y_i is the gross output and K_i is the capital stock. We will study this system for the set of parameters

$$A = 5,\ C = 25,\ D = 0.015,\ E = 0.05,\ G = 320,\ H = 7,\ \alpha = 5,$$

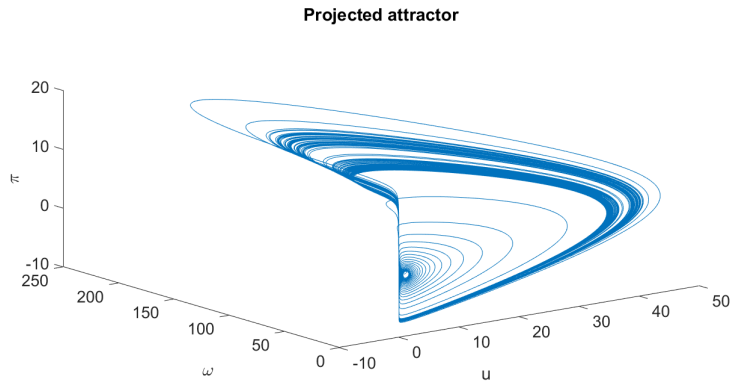

Figure 4: A projection of the Asada et al. attractor onto the (u, ω, π)-plane. It is calculated with $N = 800,000$ time steps with size $\Delta t = 0.005$ using the `MATLAB`-function `ode45`.

$$\delta_1 = 0.05,\ \ \delta_2 = 0.0505,\ \ \delta_3 = 0.051, \epsilon = 0.00001,\ \ s = 0.29 \text{ and}$$

$$b_{12} = b_{13} = b_{23} = 0.015,$$

which slightly differs from the set H.-W. Lorenz studied. The initial values are $K_0 = 393$ and $Y_0 = 63$ for all three sectors [11]. We show the results for this set of parameters and for the original set with $H = 3$.

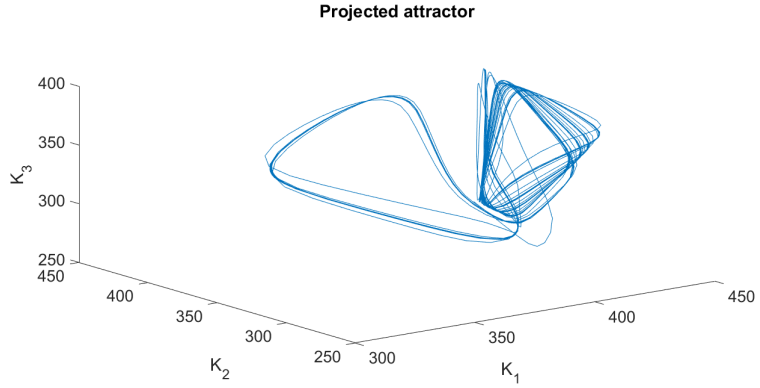

Figure 5: A projection of the H.-W. Lorenz attractor for $H = 3$ onto the (K_1, K_2, K_3)-plane. It is calculated with $N = 20,000$ time steps with size $\Delta t = 1$ using a fourth order Runga-Kutta method. We see a complex, messy structure. For the original set of parameters, we found the same attractor as H.-W. Lorenz.

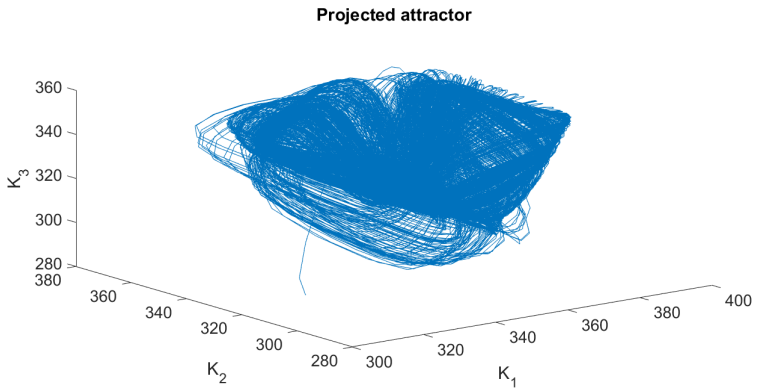

Figure 6: A projection of the H.-W. Lorenz attractor for $H = 7$ onto the (K_1, K_2, K_3)-plane. It is calculated with $N = 20,000$ time steps with size $\Delta t = 1$ using a fourth order Runga-Kutta method.

3.1 Lyapunov exponents

In this section, we demonstrate the convergence of the Lyapunov exponents for the four-dimensional Asada et al. model. We list the Lyapunov exponents for each model.

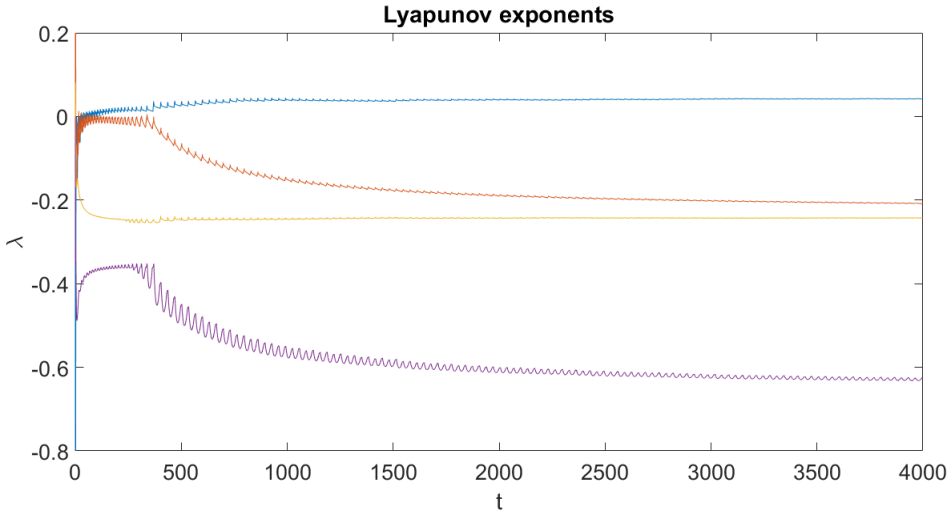

Figure 7: Plot of $\frac{1}{t}\int_0^t B_{ii}(s)ds$ as in (6) for the four-dimensional Asada et al. model versus time t. The limiting behavior determines the value of the Lyapunov exponents. Small oscillations occur but there appears to be convergence for each Lyapunov exponent.

Table 1: Lyapunov exponents λ_i

Lyapunov exponent	Lorenz-63	Medio	Asada et al.	H.-W. Lorenz for $H = 3$	H.-W. Lorenz for $H = 7$
λ_1	1.0949	0.2772	0.0427	-0.0002	0.0088
λ_2	-0.1328	-0.0006	-0.2070	-0.0052	-0.0010
λ_3	-15.6843	-2.9753	-0.2423	-0.0885	-0.0185
λ_4	-	-4.5471	-0.6264	-0.2650	-0.1810
λ_5	-	-8.9307	-	-0.2831	-0.2349
λ_6	-	-11.0678	-	-0.3224	-0.3204
λ_7	-	-15.4458	-	-	-
λ_8	-	-17.0468	-	-	-
λ_9	-	-19.9864	-	-	-
λ_{10}	-	-20.2784	-	-	-

The Lyapunov dimensions are 2.0613 for the Lorenz-63 model, 2.0930 for the Medio model, 1.2062 for the Asada et al. model, 0 for the H.-W. Lorenz model ($H = 3$) and 2.4179 for the H.-W. Lorenz model ($H = 7$). We expect that the positive Lyapunov exponent for the Asada et al. model should be zero. We conclude that the models Lorenz-63, Medio and H.-W. Lorenz ($H = 7$) are chaotic, whereas Asada et al. and H.-W. Lorenz ($H = 7$) apparently are not.

3.2 Unstable periodic orbits

The Lindstedt-Poincaré method as described by Viswanath is successfully implemented for the Duffing oscillator and the Lorenz-63 model. For the Duffing oscillator, the first two iterations give the same results as in [13]. For the Lorenz-63 model, we found the smallest residual error to be $8.6e-8$.
It turned out to be problematic to find good starting conditions for the iteration. For the three economic models, we unsuccessfully tried to implement the method from a starting point on the attractor. No convergence was found. Consequently, we were unable to draw any conclusions about economic models by studying unstable periodic orbits.

Table 2: Lindstedt-Poincaré method

(a) Duffing oscillator. The starting guess is $(q, \dot{q}) = (\cos(t), \sin(t))$.

iteration	Real residual error
0	1e-1
1	2.3e-3
2	9.2e-7
3	3.1e-13
4	1.6e-13
5	1.0e-13
6	7.1e-14

(b) Lorenz-63 model. The starting guess is $(x_0, y_0, z_0) = (-13.8, -19.6, 27.0)$.

iteration	Real residual error
0	2.0e0
1	3.5e-6
2	2.7e-8
3	3.4e-8
4	4.7e-8
5	6.4e-8
6	8.6e-8

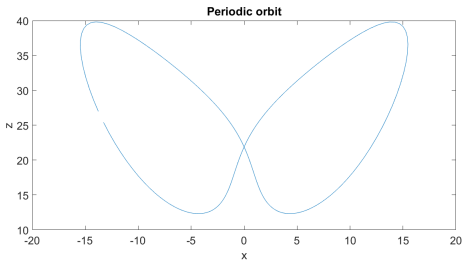

Figure 8: Projection in the (x, z)-plane of the periodic orbit of the Lorenz-63 model calculated with the Lindstedt-Poincaré method.

3.3 The 0-1 test for chaos

We implemented the 0-1 test for chaos for the three economic models. For comparison, the 0-1 test is also applied to the Lorenz-63 model.

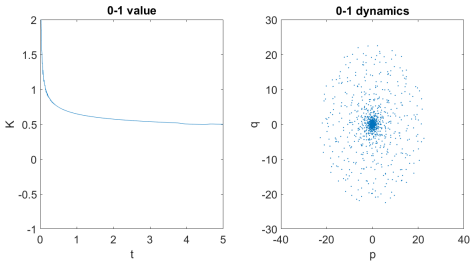

Figure 9: 0-1 test for chaos for the Asada et al. model. Left: limiting behavior of the K-value. Right: plot of $p_c(n)$ and $q_c(n)$ for $n \leq N/10$ and a random value of $c \in (\pi/5, 4\pi/5)$.

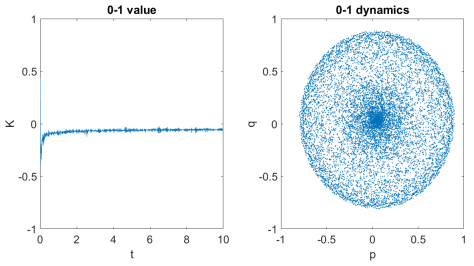

Figure 10: 0-1 test for chaos for the Medio model. Left: limiting behavior of the K-value. Right: plot of $p_c(n)$ and $q_c(n)$ for $n \leq N/10$ and a random value of $c \in (\pi/5, 4\pi/5)$.

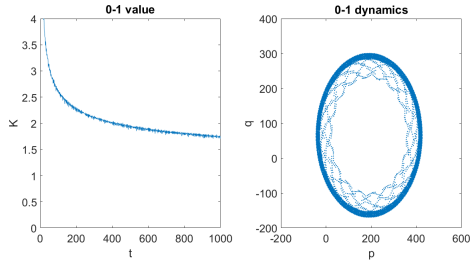

Figure 11: 0-1 test for chaos for the H.-W. Lorenz model with $H = 3$. Left: limiting behavior of the K-value. Right: plot of $p_c(n)$ and $q_c(n)$ for $n \leq N/10$ and a random value of $c \in (\pi/5, 4\pi/5)$.

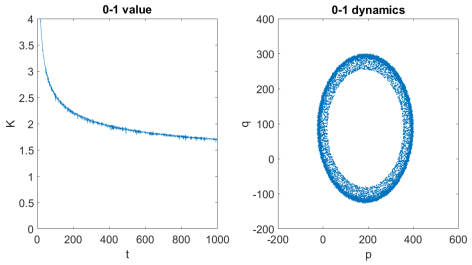

Figure 12: 0-1 test for chaos for the H.-W. Lorenz model with $H = 7$. Left: limiting behavior of the K-value. Right: plot of $p_c(n)$ and $q_c(n)$ for $n \leq N/10$ and a random value of $c \in (\pi/5, 4\pi/5)$.

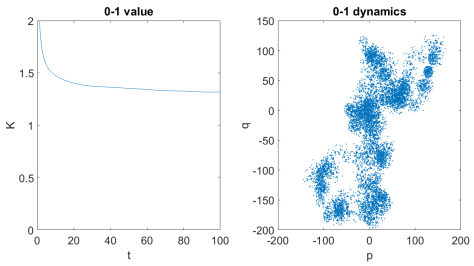

Figure 13: 0-1 test for chaos for the Lorenz-63 model. Left: limiting behavior of the K-value. Right: plot of $p_c(n)$ and $q_c(n)$ for $n \leq N/10$ and a random value of $c \in (\pi/5, 4\pi/5)$.

Based on the 0-1 test for chaos, we find the H.-W. Lorenz model for both cases exhibiting chaos, whereas the Medio model does not exhibit chaos. We were unable to draw conclusions for the Asada et al. model.

4 Conclusions

To validate our methods, we tested the Duffing oscillator and the Lorenz-63 model with the analysis of Lyapunov exponents and the calculation of periodic orbits using the Lindstedt-Poincaré method as described by Viswanath. We found the expected results for both methods. The Lyapunov dimension of 2.0613 seems to be within a small margin of the results in other studies. The Lindstedt-Poincaré method gives a convergence to a real residual error of 8.6e-8 for the Lorenz-63 model. We expected to find (unstable) periodic orbits.
The Medio model has one strictly positive Lyapunov exponent $\lambda_1 = 0.2772$. Its Lyapunov dimension is bigger than the dimension of the Lorenz-63 model, suggesting it is "more chaotic" than the Lorenz-63 model. However, the K-value clearly converges to zero, which suggest that the system does not exhibit chaotic behavior. Our results are inconclusive.
In the Asada et al. model, we found one positive Lyapunov exponent $\lambda_1 = 0.0427$. It may be that this value should be zero, as the 0-1 test for chaos does not give a satisfying conclusion. Our results are inconclusive.
The H.-W. Lorenz model for $H = 3$ has no positive Lyapunov exponent and

the model for $H = 7$ has one positive Lyapunov exponent and the biggest Lyapunov dimension of all systems studied in this thesis. However, the 0-1 test for chaos gives the same results for both sets of parameters. This is obviously in disagreement with the results for the analysis of Lyapunov exponents. The case $H = 7$ satisfies both conditions and the case $H = 3$ is inconclusive.

Overall there seems to be a difference between the results from the analysis of Lyapunov exponents and the 0-1 test for chaos. As the results of the study of Lyapunov exponents and Lyapunov dimension have been confirmed in many papers, we think the 0-1 test for chaos has to be investigated more thoroughly to understand the conflicting results of this thesis. The method of computing unstable periodic orbits has shown to be a good method for systems for which good starting conditions can be determined. In other cases, it turned out to be problematic to find initial values in the basin of attraction of the unstable periodic orbit.

References

[1] Asada, T., Flaschel, P., Proaño, C.R. and Groh, G., *Continuous Time, Period Analysis and Chaos from an Empirical Perspective*, CEM Working Paper 144, Bielefeld University, 2007

[2] Devaney, R.L., *An Introduction to Chaotic Dynamical Systems*, Addison-Wesley, 1989

[3] Dieci, L., Jolly, M.S. and Van Vleck, E.S., *Numerical techniques for approximating Lyapunov exponents and their implementation*, Journal of Computational and Nonlinear Dynamics, 6(1):011003, 2011

[4] Frank, J., *Lecture Notes on Lyapunov Exponents*, 2016

[5] Gottwald, G.A. and Melbourne, I., *The 0-1 Test for Chaos: A review*, SIAM Journal on Applied Dynamical Systems, 8 (1), pp. 129-145, 2009

[6] Guckenheim, J. and Meloon, B., *Computing Periodic Orbits and their Bifurcations with Automatic Differentiation*, Mathematics Department Ithaca New York, 1999

[7] Hommes, C., *Behavioral Rationality and Heterogeneous Expectations in Complex Economic Systems*, Cambridgde University Press, 2013

[8] Kaplan, J.L. and Yorke, J.A., *Chaotic Behavior of Multidimensional Difference Equations, in Functional Differential Equations and Approximations of Fixed Points*, edited by H.-O. Peitgen and H.-O. Walter, Lecture Notes in Mathematics, 730 (Springer, Berlin, 1979b), p. 204.

[9] Kaldor, N., *A model of the trade cycle*, Economic Journal, vol. 50, pp. 78-90, 1940

[10] Lorenz, E.N., *Deterministic non-periodic flows*, J. Atmos. Sci., vol. 20, pp. 130-141, 1963

[11] Lorenz, H.-W., *Strange attractors in a Multisector Business Model*, Journal of Economic Behavior and Organization, vol. 8, issue 3, pp. 397-411, 1987

[12] Medio, A., *Discrete and Continuous-Time Models of Chaotic Dynamics in Economics*, Structural Change and Economic Dynamics, vol. 2, no. 1, pp. 99-118, 1991

[13] Viswanath, D., *The Lindstedt-Poincaré Technique as an Algorithm for Computing Periodic Orbits*, SIAM Review, vol. 43, no. 3, pp. 478-495, 2001